Autoimmune receptor encephalitis in ApoE$^{-/-}$ mice induced by active immunization with NMDA1

LIMING YU[1,2], YUJUN WEN[3], JUAN YANG[4], GUOWEI WANG[1], NA ZHANG[1], XINLEI GAO[5], JIAYU GUO[6] and ZHENHAI WANG[4,7,8]

[1]School of Clinical Medicine, Ningxia Medical University, Yinchuan, Ningxia 750001; [2]Department of Neurology, Huangshi Central Hospital, Affiliated Hospital of Hubei Polytechnic University, Edong Healthcare Group, Huangshi, Wuhan 435000; [3]Ningxia Key Laboratory of Cerebrocranial Diseases, Ningxia Medical University, Yinchuan, Ningxia 750001; [4]Neurology Center, General Hospital of Ningxia Medical University, Yinchuan, Ningxia 750004; [5]Department of Neurology, Shenmu Hospital, Yulin, Shanxi 719000; [6]Department of Neurology, People's Hospital of Ningxia Hui Autonomous Region; [7]Institute of Medical Sciences, General Hospital of Ningxia Medical University; [8]Diagnosis and Treatment Engineering Technology Research Center of Nervous System Diseases of Ningxia Hui Autonomous Region, Yinchuan, Ningxia 750004, P.R. China

Received April 3, 2023; Accepted September 29, 2023

DOI: 10.3892/mmr.2023.13120

Abstract. Subacute progressive neuropsychiatric symptoms with cognitive and motor impairment and autoimmune seizures are some of the typical symptoms of anti-N-methyl-D-aspartate receptor (anti-NMDAR) encephalitis. The mechanisms underlying this disease are yet to be elucidated, which could be partly attributed to the lack of appropriate animal models. The present study aimed to establish an active immune mouse model of anti-NMDAR encephalitis. Mice were immunized with the extracellular segment of the NMDA1 protein, then subjected to open-field and novel object recognition experiments. Plasma was collected after euthanasia on day 30 after immunization and anti-NMDA1 antibodies were detected using ELISA. Furthermore, brain slices were analyzed to measure postsynaptic density protein 95 (PSD-95) and NMDA1 expression. Western blot analysis of NMDA1 and PSD-95 protein expression levels in the hippocampus was also performed. In addition, protein expression levels of PSD-95 and NMDA1 in mouse neuronal HT-22 cells were evaluated. Compared with controls, mice immunized with NMDA1 exhibited anxiety, depression and memory impairment. Moreover, high anti-NMDA1 antibody titers were detected with ELISA and the levels of anti-NMDA1 antibody reduced postsynaptic NMDA1 protein density in the mouse hippocampus. These findings demonstrated the successful construction of a novel mouse model of anti-NMDAR encephalitis by actively immunizing the mice with the extracellular segment of the NMDA1 protein. This model may be useful for studying the pathogenesis and drug treatment of anti-NMDAR encephalitis in the future.

Correspondence to: Dr Zhenhai Wang, Institute of Medical Sciences, General Hospital of Ningxia Medical University, 804 Shengli South Street, Yinchuan, Ningxia 750004, P.R. China
E-mail: nyfywzh@163.com

Abbreviations: NMDAR, N-methyl-D-aspartate receptor; NMDA1, N-methyl-D-aspartate receptor subunit 1; PSD-95, postsynaptic density protein 95; NR1, N-methyl-D-aspartate receptor subunit 1; GluN2B, N-methyl-D-aspartate receptor subunit 2B; GluN1, N-methyl-D-aspartate receptor subunit 1; GRIN1, N-methyl-D-aspartate receptor subunit 1; ATD, amino-terminal domain; CFA, complete freund's adjuvant; NOR, new object experiment; OFT, open field test

Key words: anti-N-methyl-D-aspartate receptor encephalitis, active immunization, N-methyl-D-aspartate receptor subunit 1, novel object recognition, open field experiments

Introduction

Anti-N-methyl-D-aspartate receptor (anti-NMDAR) encephalitis, originally described as limbic encephalitis, is characterized by seizures, dyskinesia, behavioral changes, mood disturbances, cognitive impairment, autonomic dysfunction and altered levels of consciousness (1). Anti-NMDAR antibodies in serum react with the N-terminal domain of N-methyl-D-aspartate receptor subunit 1 (NMDAR1; also known as NR1, GRIN1 or GluN1) subunit of NMDAR. This interaction results in the internalization of neuronal cell surface receptors, reduced cell surface and synaptic NMDAR levels and symptoms such as memory and behavioral changes (2,3). However, the pathogenic mechanisms underlying anti-NMDAR encephalitis are poorly understood.

To comprehensively evaluate anti-NMDAR encephalitis, an animal model of the disease is necessary. A previous study performed by Planagumà *et al* (3) continuously perfused cerebrospinal fluid from patients with anti-NMDAR encephalitis into the ventricles of mice, which resulted in progressive memory deficits, anhedonia and depression-like behaviors.

This was the first proof of concept study that demonstrated a mouse model could be generated using autoantibodies from patients with autoimmune encephalitis. Subsequently, Jones *et al* (4) reported for the first time in 2019 the immunization of C57BL/6 mice with purified GluN1/GluN2B NMDA fully assembled tetrameric receptors embedded in NMDA receptor proteoliposomes. Linnoila *et al* (5) inoculated six mice intranasally with the herpes simplex virus and reported that four of these mice developed serum NMDAR antibodies. A decrease in the NMDAR protein expression level in the hippocampal postsynaptic membrane of the mice was reported. Pan *et al* (6) actively immunized ApoE$^{-/-}$ mice with NMDAR peptides to produce a large amount of serum NMDAR antibodies. Ding *et al* (7) successfully constructed an anti-NMDAR encephalitis model by actively immunizing female C57BL/6 mice with the amino-terminal domain (ATD) peptide (GluN1356-385) of the GluN1 protein subunit. At present, there are few studies on the construction of anti-NMDAR encephalitis mouse models and there is scope for exploring how such models could be built to better replicate the clinical manifestations of the disease.

In the present study, C57 ApoE$^{-/-}$ mice were immunized with prokaryote-expressed human NMDA1 protein, and an anti-NMDAR encephalitis mouse model was successfully constructed, which was confirmed using ELISA, western blotting, behavioral experiments and immunofluorescence.

Materials and methods

Protein expression and purification. The NMDA1 (19-559 aa) gene was inserted into the expression vector pET30a by whole gene synthesis using the restriction enzyme digestion sites NdeI and HindIII, and the accuracy of the final expression vector was confirmed by enzyme digestion and Sanger sequencing (Sangon Biotech Co., Ltd.). Finally, it was introduced into the bacterial host *Escherichia coli* Rosetta blue (DE3). The expression of NMDA1 (19-559 aa) protein was induced using 0.2 mmol/l Isopropyl-β-D-1-thiogalactoside (IPTG) and 50 ug/ml kanamycin at 15˚C for 16 h, and then NMDA1 (19-559 aa) protein was expressed as a form of inclusion body. Subsequently, the fraction with the inclusion bodies was dissolved in the solubilization buffer (10 mM Tris-HCl, 100 mM sodium phosphate, 6 M guanidine-HCl, 10 mM imidazole, 2 mM 2-mercaptoethanol, pH 8.0) and the clarified supernatant was run through a 45-165 μm Ni-IDA column (cat. no. C600292, Sangon Biotech Co., Ltd.) for purification of His-tagged protein. Elution buffers including different concentrations of imidazole (50 mM Tris; 300 mM NaCl; 50, 100 or 300 mM Imidazole; pH 8.0) were used to elute the His-tagged protein. The purity of NMDA1 (19-559 aa) in the eluted solutions was assessed using 10% SDS-PAGE and the gels were stained using Coomassie Brilliant Blue R-250 (cat. no. 1610436; Bio-Rad Laboratories) according to the manufacturer's protocols. Consequently, we chose the concentration of 300 mM imidazole as the elution condition for the subsequent protein purification (8,9).

Mouse immunization. C57BL/6 mice (age, 12 weeks; female; ApoE$^{-/-}$; n=10) were immunized with a mixture of NMDA1 (19-559 aa; Nanjing MerryBio Co., Ltd.) and OVA peptide (cat. no. HY-P1489A; MedChemExpress) emulsified in an equal volume of complete Freund's adjuvant [*Mycobacterium tuberculosis* H37RA (cat. no. 231141; Becton, Dickinson and Company) plus incomplete Freund's] at a final concentration of 1 mg/ml. The right groin of each of the animals in the NMDA1 treatment group (n=5) was subcutaneously injected with 100 μg of NMDA1 peptide and 20 μg of OVA. The control mice (n=5) received an emulsion mixture of OVA and CFA (cat. no. F5881; MilliporeSigma) and an equal volume of 0.9% NaCl. All mice were injected intraperitoneally with 200 ng pertussis toxin (cat. no. B7273; APExBIO Technology LLC) on the day of the last immunization and again 48 h later. All mice were housed in a 12 h light/dark cycle at 24˚C with 60% humidity and *ad libitum* access to food and water The animal study was reviewed and approved by the Laboratory Animal Ethical and Welfare Committee of Laboratory Animal Center, Ningxia Medical University (Yinchuan, China; approval no. IACUC-NYLAC-2019-072).

Euthanasia of mice. Mice were placed in a euthanasia box, which was then infused with CO_2 at a rate of 30% vol/min. Animals were observed for 3 min to confirm death. The heartbeat was observed, respiration was monitored and pupil dilation was assessed to ensure successful animal euthanasia. Heart blood and brain tissue were then collected for further experimental use and the rest of the remains of the mice were disposed of by the Experimental Animal Center of Ningxia Medical University within 1 week.

Neuronal cell culture. HT-22 immortalized mouse hippocampal cells were purchased from Procell Life Science & Technology Co., Ltd. HT-22 cells were cultured and maintained in Dulbecco's modified Eagle's medium supplemented with 10% FBS, 100 units/ml penicillin and 100 μg/ml streptomycin at 37˚C in humidified conditions under 5% CO_2. The medium was changed thrice weekly and cultures were split in a ratio of 1:5 weekly.

Behavioral assessments. Mice were transferred to the behavioral analysis room a day before observational experiments to allow them to adapt to the environment. All devices were cleaned before the experiments. For the open field test (OFT), the experimental area was classified into a central area (25% of the total area) and a peripheral area (75% of the total area). The mice were placed in the center of the open field and the behavioral parameters were recorded for 5 min using a video tracking system (Smart 3.0; Panlab). Next, the new object experiment (NOR) was performed. The mice were placed into a box for 5 min with two identical objects and taken out to rest for 1 h. Then, one of the objects was replaced with an object of the same material but different shapes and colors and the experiment continued for 5 min. Exploratory behavior was classed as the mouse nose tip being within 2 cm of the object. The video tracking system was used to record the time during which the mouse explored the new and old objects separately. In addition, the NOR index was calculated as follows: Percentage of time spent on new objects/total time spent on both objects. After each mouse experiment, the box was cleaned and ethanol was used to remove residual odors.

ELISA. Plasma collected from mouse hearts after the euthanasia of animals was stored at -80˚C. ELISA plates (96-wells) were coated with 0.5 μg of NMDA1 protein in 100 μl PBS/well overnight at 4˚C and blocked with 10% FBS/PBS with 0.1% Tween20 (cat. no. 04-001-1A; Biological Industries; Sartorius AG). Then, the mouse plasma (1:1,000; 100 μl/well) was added to the wells for 2 h at 37˚C. The signal was amplified with HRP-linked goat anti-mouse IgG antibodies (1:5,000; 100 μl/well; cat. no. A21010; Abbkine Scientific Co., Ltd.). Absorbance was measured at 450 nm using a microplate reader.

Immunoblotting analyses. Hippocampi were dissected from the thawed brain and lysed in RIPA buffer (cat. no. KGP250; Nanjing KeyGen Biotech Co., Ltd.). Protein concentration in the lysates was determined by the using the BCA method according to the manufacturer's protocols (cat. no. KGP902; Nanjing KeyGen Biotech Co., Ltd.). Then, 80 μg of whole protein was denatured at 100˚C for 5 min. Protein (80 μg) was separated on 10% Mini-Protean TGX gels and subsequently transferred onto a PVDF membrane. After blocking with 5% BSA (cat. no. A6010A; Biotopped Life Sciences) for 30 min at 25˚C, the membranes were incubated with NMDA1 (1:1,000; cat. no. ab134308; Abcam), postsynaptic density protein 95 (PSD-95; 1:1,000; cat. no. ab18258; Abcam) and GAPDH antibodies (1:1,000; cat. no. TA802519; OriGene Technologies, Inc.) overnight at 4˚C. The membrane was washed thrice with TBST (0.1% Tween-20 in TBS) and incubated with Dylight 680 goat anti-rabbit IgG (1:1,000; cat. no. A23720; Abbkine) and IRDye 800CW goat anti-mouse IgG antibodies (1:2,000; cat. no. 926-32210; LI-COR Biosciences) for 1 h at 37˚C. Protein bands were visualized using the Odyssey CLx imager (LI-COR Biosciences). The grayscale value of the protein was semi-quantified using ImageJ (version 1.53c; National Institutes of Health).

Immunofluorescence. For the determination of antibodies bound to brain tissues by immunofluorescence, 20 μm coronal sections were blocked using 10% normal goat serum (Wuhan Boster Biological Technology Ltd.) for 60 min at room temperature, incubated overnight at 4˚C with NMDA1 antibodies (1:100) and visualized after staining with DyLight 488 goat anti-mouse IgG (1:500; cat. no. A23210; Abbkine) for 30 min at 37˚C. Then, the tissue sections were first incubated overnight at 4˚C with PSD-95 antibodies (1:100; cat. no. ab18258; Abcam) and then incubated with the DyLight 680 goat anti-rabbit IgG antibodies (1:500; cat. no. A23720; Abbkine) for 30 min at 37˚C. The slides were mounted and scanned using a DM6 fluorescence microscope (Leica Microsystems GmbH). HT-22 cells (1x10^5 cells/ml) were incubated in 24 well plates with NMDA1 antibodies (20 ng/μl) or mouse plasma (0.1 μl/μl) at 37˚C for 24 h. The cells were then fixed with 100% methanol at -20˚C for 5 min, blocked with 10% normal goat serum for 30 min at room temperature, incubated overnight at 4˚C with NMDA1 antibodies (1:100) and visualized after staining with the DyLight 488 goat anti-mouse IgG (1:500; cat. no. A23210; Abbkine) for 30 min at 37˚C. Then, the slides were incubated overnight at 4˚C with PSD-95 antibodies (1:100) and incubated with the DyLight 680 goat anti-rabbit IgG antibodies (1:500) for 30 min at 37˚C. The slides were then mounted and imaged using a fluorescence microscope (Zeiss). The protein cluster density was analyzed using the 'colocalization' and 'spot' functions of the Imaris software (version 9.0.1; Oxford Instruments).

Statistical analysis. The data of each group were tested for normality and homogeneity of variance. An unpaired Student's t-test, one-sample t-test and Welch's t-test was performed for comparison between two groups. A two-way ANOVA followed by Sidak's post hoc test was performed for comparisons between multiple groups. P<0.05 was considered to indicate statistical significance. Data are presented as mean ± standard error of the mean, all experiments were performed three times. Statistical analyses were performed using GraphPad Prism software (version 8; Dotmatics).

Results

NMDA1 caused behavioral changes in mice. To study the behavioral alterations in mice treated with NMDA1, OFTs were performed on days 7, 16 and 25 after immunization and NORs were performed on days 9, 18 and 27 after immunization (Fig. 1A). The open-field loci of the mice in the control (CON) and NMDA1 groups were measured (Fig. 1B and C). Compared with the CON group, the total horizontal movement distance of the NMDA1 group significantly decreased on day 16 after immunization (P<0.01) (Fig. 1D). Moreover, the time in the central area was significantly reduced in NMDA1-treated mice compared with CON mice on days 16 and 25 after immunization (P<0.05 and P<0.01, respectively) (Fig. 1E). The aforementioned results demonstrated that the mice in the NMDA1 group exhibited greater anxiety and depression compared with those in the CON group.

Healthy mice tend to explore new objects, hence, the recognition index exhibited by these mice would be >50%. However, mice with impaired memory cannot recognize new or old objects, therefore, the recognition index of these mice would be ~50% (10). On days 9, 18 and 27 after immunization, the NOR index in the CON group was >50% and was significantly greater than the expected 50% (P<0.01, P<0.05 and P<0.05, respectively); however, there was no significant difference between the NOR and the expected 50% in the NMDA1 group over the three days (Fig. 1F). The movement trajectory diagram of the mouse NOR was recorded, the mouse in the CON group spent longer exploring a new object than an old object (Fig. 1G). The aforementioned results demonstrated that compared with the mice in the CON group, those in the NMDA1 group demonstrated memory impairment.

Production of plasma anti-NMDA1 antibodies reduced the protein expression levels of the hippocampal, NMDA1 protein. Anti-NMDA1 antibody levels in mouse plasma were assessed using ELISA (Fig. 2A). Compared with the CON group, the level of anti-NMDA1 antibodies in the plasma of the mice in the NMDA1 group was significantly increased (P<0.001).

Western blotting was used to assess the protein expression levels of NMDA1 and PSD-95 proteins in the mouse hippocampus (Fig. 2B-D). These results demonstrated that compared with the CON group, the protein expression levels of the NMDA1 protein were significantly decreased in the

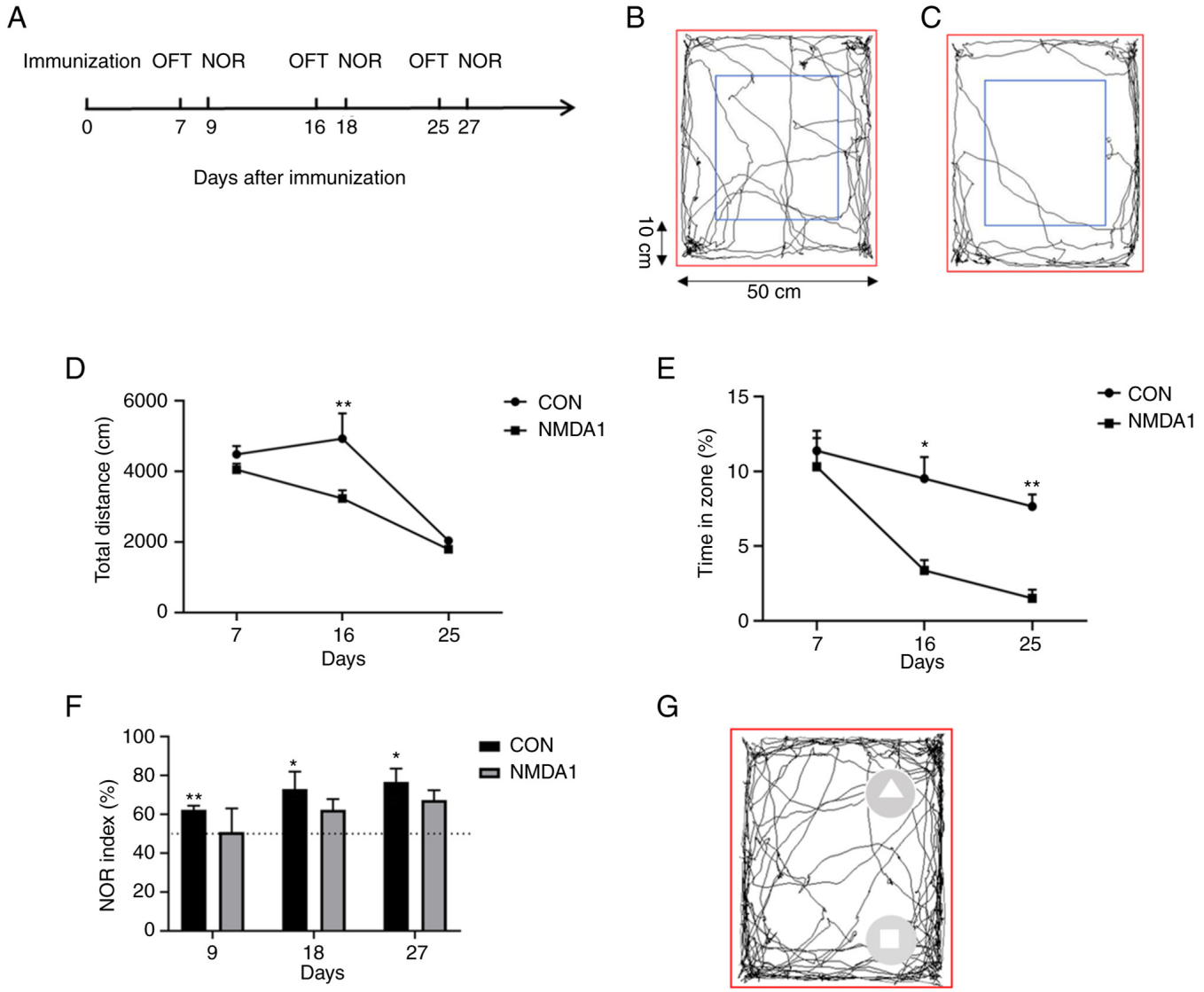

Figure 1. Behavioral changes were observed in mice after immunization with NMDA1. (A) OFT were performed on days 7, 16 and 25 after immunization, while NOR experiments were performed on days 9, 18 and 27 after NMDA1 immunization. Movement trajectories of the mice were measured in a 50x50 cm area (red box), an area 10 cm from the edge of the area (blue box, central area) and the area between the red and blue boxes (peripheral area) in (B) CON mice and (C) NMDA1-treated mice. (D) The total distance moved by mice in the NMDA1 and CON groups. *P<0.05, **P<0.01 vs. CON. (E) Time spent in the central region of the NMDA1 and CON groups. *P<0.05, **P<0.01 vs. CON. (F) Recognition index of mice in the NMDA1 and CON groups. *P<0.05, **P<0.01 vs. 50%. (G) Mouse movement trajectory map, square represents an old object and a triangle represents a new object. Data are presented as mean ± standard error of the mean. n=5. OFT, open field experiments; NOR, novel object recognition experiments; NMDA1, N-methyl-D-aspartate receptor subunit 1; CON, control.

NMDA1 group (P<0.05). However, there was no significant difference in the expression levels of the PSD-95 protein between the two groups.

Production of anti-NMDA1 antibodies reduced the protein expression levels of NMDA1 in the mouse hippocampal postsynaptic membrane. To evaluate the effect of anti-NMDA1 antibodies in mouse plasma on the expression of the NMDA1 protein in the hippocampus, frozen tissue section immunofluorescence imaging was used to detect the protein expression levels of NMDA1 and PSD-95 in the mouse hippocampus. Immunolabeling of NMDA1 and PSD-95 proteins in the hippocampus of mice in the CON and NMDA1 groups was performed (Fig. 3A) and a representative 2D image of the CA3 region and the density analysis of protein clusters was obtained (Fig. 3B). The total cluster density of NMDA1 protein in the hippocampus of the mice in the CON group was significantly higher compared with the mice in the NMDA1 group (P<0.05; Fig. 3C). However, the total cluster density of PSD-95 protein in the hippocampus of the mice in the CON group was not significantly different compared with the NMDA1 group (Fig. 3D). When the NMDA1 protein in the hippocampal synapse of the mice was examined, the cluster density in the CON group was significantly higher compared with the NMDA1 group (P<0.05; Fig. 3E).

Reduction in the expression of the NMDA1 protein in the HT-22 cellular postsynaptic membrane by the production of anti-NMDA1 antibodies. To determine the effect of anti-NMDA1 antibodies on the expression levels of NMDA1 and PSD-95 proteins in neuronal synapses,

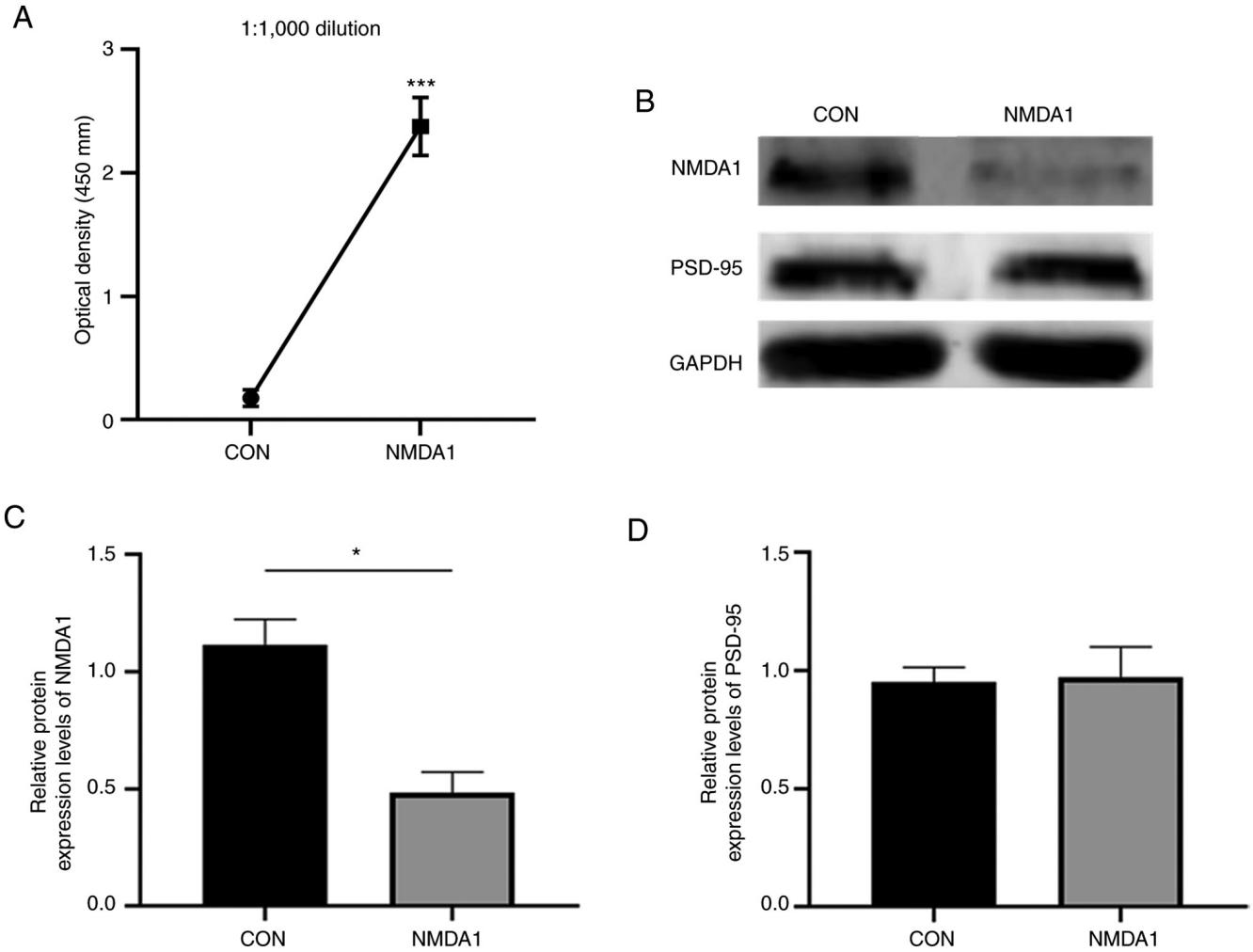

Figure 2. Production of NMDA1 antibodies and reduction of hippocampal NMDA1 protein expression levels in mouse plasma. (A) ELISA detection of anti-NMDA1 antibody levels in mouse plasma, n=5. (B) Western blotting of NMDA1 and PSD-95 proteins in each group of mice and protein expression levels of (C) NMDA1 and (D) PSD-95 in CON and NMDA1-treated mice, n=3. *P<0.05, ***P<0.001 vs. CON. Data are presented as mean ± standard error of the mean. CON, control; NMDA1, N-methyl-D-aspartate receptor subunit 1; PSD-95, postsynaptic density protein 95.

immunofluorescence was used to evaluate the protein expression levels of NMDA1 and PSD-95 in HT-22 cells (Fig. 4A). The number of protein clusters of NMDA1 and PSD-95 and the number of synaptic clusters of NMDA1 immunolabeled were quantified (Fig. 4B-D). The number of protein clusters of NMDA1 in the PBS group was significantly higher compared with the NMDA1 Ab group (P<0.05). The total PSD-95 number of protein clusters in the PBS group was not significantly different compared with the NMDA1 Ab group. The number of synaptic NMDA1 clusters in the PBS group was significantly higher compared with the NMDA1 Ab group (P<0.05). After adding mouse plasma to the cultured HT-22 cells, the number of clusters of NMDA1 and PSD-95 proteins and the number of synaptic clusters of NMDA1 were immunolabeled (Fig. 4E). The number of clusters of NMDA1 in the CON group was significantly higher compared with the NMDA1 group (P<0.05) (Fig. 4F). The number of clusters of PSD-95 in the CON group was not significantly different compared with the NMDA1 group (Fig. 4G). The synaptic cluster of NMDA1 protein in the CON group was significantly higher compared with the NMDA1 group (P<0.05) (Fig. 4H).

Discussion

The results of the present study demonstrated that active immunization of mice with the NMDA1 (19-559 aa) protein induced a disease state that exhibited the major features of human anti-NMDAR encephalitis, such as abnormal behavior, cognitive dysfunction or memory deficit (11). The establishment of animal models via active immunization has previously served a key role in the research of neurological diseases (12). For example, peptide fragments extracted from myelin sheaths have previously been used to generate experimental autoimmune encephalomyelitis (13). Similarly, active immunization with neuromuscular junction proteins has been reported to result in myasthenia-like features in mice (14). Earlier studies have reported that active immunization of ApoE$^{-/-}$ mice with NMDA1 peptide fragments resulted in high levels of circulating anti-NMDA1 antibodies and induced psychotic-like symptoms, such as hyperactivity, upon MK-801 challenge (6,15). The present study demonstrated that active immunization with the NMDA1 protein induced high titers of pathogenic anti-NMDA1 autoantibodies. Furthermore, this immunization reproduced many of the typical symptoms of

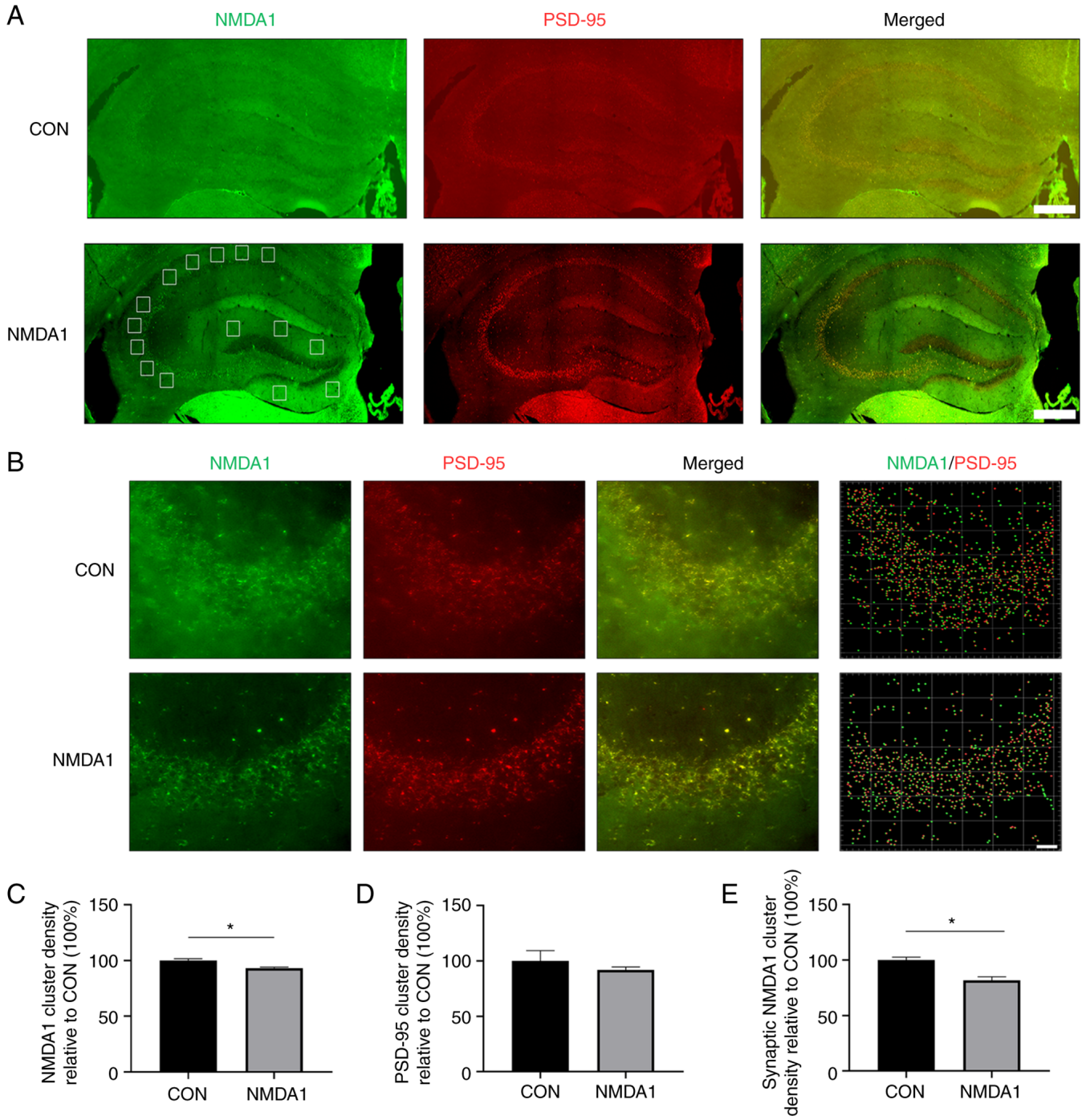

Figure 3. NMDA1 antibodies reduce NMDA1 protein expression levels in the mouse hippocampal postsynaptic membrane. (A) Immunolabeling of NMDA1 protein (green) and PSD-95 protein (red) in the hippocampus of mice in the CON and NMDA1 groups. The white boxes in the NMDA1 group represent the analysis area. Scale bar, 400 μm. (B) 2D image of a representative CA3 region of the hippocampus. Scale bar, 30 μm. Cluster density was calculated as spots/1 μm^2 of (C) total clusters of NMDA1 protein, (D) total clusters of PSD-95 protein and (E) NMDA1 protein synaptic clusters, defined as protein clusters co-localized with NMDA1 and PSD-95 clusters. $^*P<0.05$ vs. CON. Data are presented as mean ± standard error of the mean. n=3. CON, control; NMDA1, N-methyl-D-aspartate receptor subunit 1; PSD-95, postsynaptic density protein 95.

anti-NMDA encephalitis in mice, such as anxiety, depression and memory loss. The model of nascent autoimmune anti-NMDA receptor encephalitis constructed in the present study may potentially provide a novel way to investigate the pathophysiology of human diseases and develop appropriate treatment methods in the future.

The NMDA1 (19-559 aa) protein was expressed and purified and it was found to exhibit good antigenicity. Subsequently, mice were immunized with NMDA1 to produce a large number of peripheral blood anti-NMDA1 antibodies. However, the triggering mechanism of the autoimmune response to the NMDA1 protein remains unclear. The epitopes of patient-derived anti-NMDA1 antibodies have previously been reported to be to be extracellular domains of the NMDA1 protein subunit (2,16-18). The use of whole protein immunogens with intact extracellular domains may have served a role in the pathogenesis of mice in the present study.

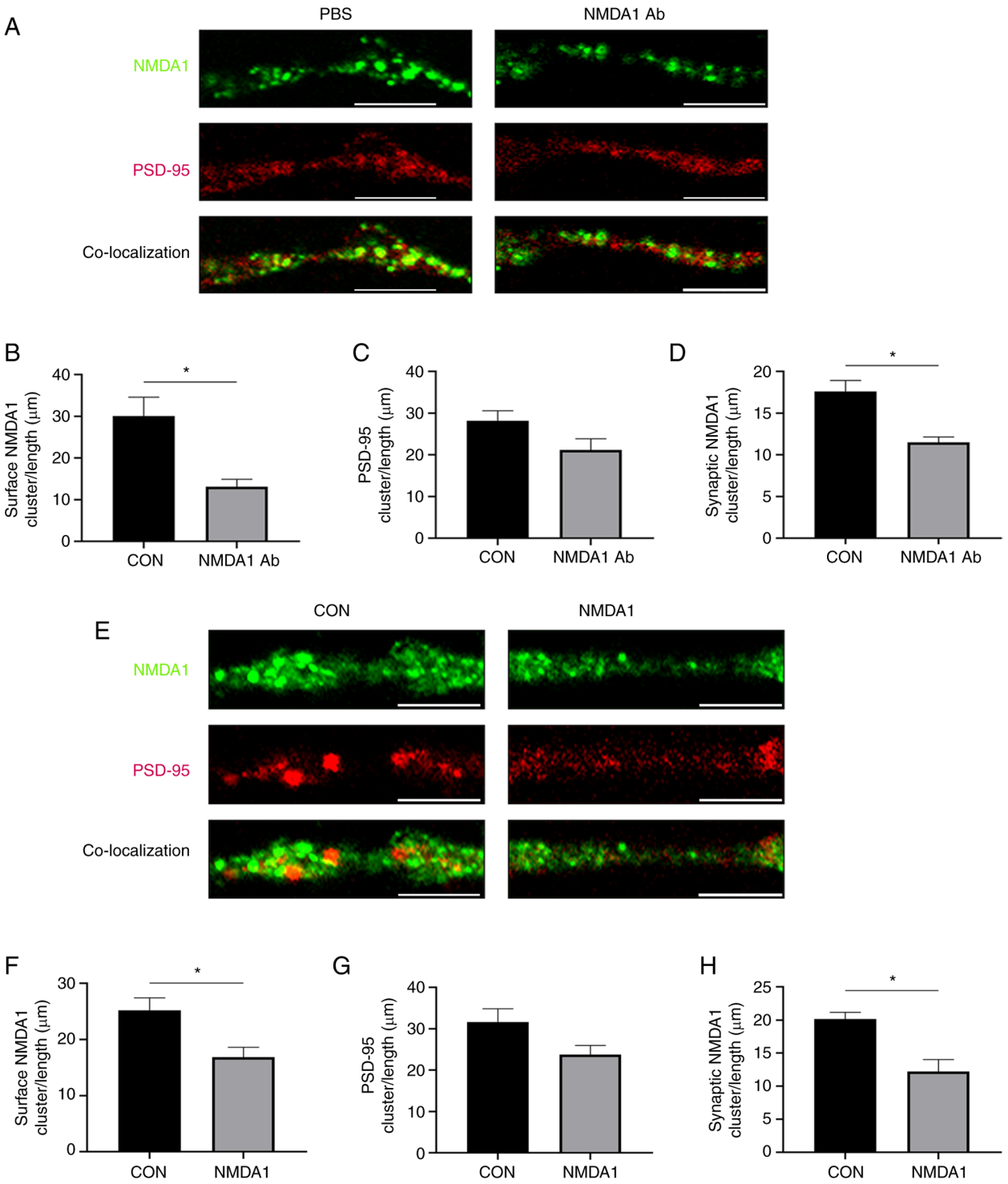

Figure 4. NMDA1 antibodies reduce NMDA1 protein expression in the HT-22 cell postsynaptic membrane. (A) Representative synapses of HT-22 cells in the PBS and the NMDA1 Ab group, demonstrating the total cluster of NMDA1 protein (green), the total cluster of PSD-95 protein (red) and the synaptic cluster of NMDA1 protein (green and red co-localized). Scale bar, 5 μm. Quantitative analysis of (B) the total cluster of NMDA1 protein in the PBS and NMDA1 Ab groups, (C) PSD-95 protein in the PBS and NMDA1 Ab groups and (D) synaptic clusters of NMDA1 protein in the PBS and NMDA1 Ab groups. (E) Representative HT-22 cell synapses in CON and NMDA1 groups. NMDA1 protein total cluster (green), PSD-95 protein total cluster (red) and NMDA1 protein synaptic cluster (green and red co-localized). Cluster density was defined as: Number of spots/the synapse length (μm). Scale bar, 5 μm. Multiple, 10x100. (F) Quantitative analysis of (F) total clusters of NMDA1 protein in the CON and NMDA1 groups, (G) total clusters of PSD-95 protein in the CON and NMDA1 groups and (H) NMDA1 protein synaptic clusters in the CON and NMDA1 groups. *P<0.05 vs. CON. Data are presented as mean ± standard error of the mean. n=3. CON, control; NMDA1, N-methyl-D-aspartate receptor subunit 1; PSD-95, postsynaptic density protein 95; Ab, antibodies; NMDAR, N-methyl-D-aspartate receptor.

Anti-NMDA1 antibodies did not directly bind to the mouse hippocampus in the present study, nonetheless, mice with high levels of plasma anti-NMDA1 antibodies exhibited reduced numbers of postsynaptic NMDA1 protein clusters in the hippocampus and reduced total hippocampal NMDA1 protein expression levels. The number of PSD-95 protein

clusters in the hippocampus remained unaltered and the same finding was demonstrated in the cellular model of NMDA1 immunization. PSD-95 is a postsynaptic scaffolding protein that serves a critical role in synaptogenesis and synaptic plasticity by providing a platform for the postsynaptic clustering of crucial synaptic proteins (19,20). PSD-95 interacts with the cytoplasmic tail of NMDA receptor subunits and shaker-type potassium channels and is required for synaptic plasticity associated with NMDA receptor signaling (19). In the present study, the reduction in the expression levels of the hippocampal NMDA1 protein suggested that these mouse antibodies were similar to patient-derived anti-NMDA1 antibodies.

Previous studies have reported that autoantibodies targeting the NMDA1 protein are involved in disease pathogenesis, such as NMDAR encephalitis (15,21). In the present study, mice demonstrated memory deficits on days 9, 18 and 27 after immunization with NMDA1. This observation was consistent with previously reported memory impairments in passive and active immunization models (3,4). Moreover, previous studies reported that treatment with anti-NMDA1 antibodies significantly reduced the density of the NMDA1 protein in the membrane of hippocampal neurons, thus impairing its function (3). Functional studies based on drug inhibition of NMDAR or hippocampal CA1-specific ablation of the GluN1 subunit have reported that hippocampal NMDAR was involved in object recognition memory (22,23). The NMDAR protein is essential for synaptic plasticity and memory formation. Anatomically, extensive synapses and interconnections are present between the limbic cortex and the hippocampus, particularly the CA1 subregion and the inferior colliculus (24) but not the dentate gyrus (25). Furthermore, several studies have reported that NMDARs located within the limbic cortex serve a pertinent role in recognition memory (26-28).

Mice exhibit thigmotaxis as they are afraid of open, unknown and potentially dangerous places. Hence, they show the characteristic of 'sticking to the wall'. It is generally believed that the more time spent in the central area of the enclosure, the lower the thigmotaxis and anxiety of the mice. Decreased total horizontal movement distance indicates depression in mice (29,30). The present study demonstrated that mice exhibited significantly reduced central area motor time and anxiety-related behaviors on days 16 and 25 after immunization with NMDA1. This finding was in accordance with the key symptoms, such as anxiety and depression, reported in patients with anti-NMDAR encephalitis (11). A previous study by Li *et al* (31) reported a shorter time spent in the center of the open area in NMDA-CSF-treated mice, but this effect was not statistically significant. However, a previous study reported a significant increase in tropism in NMDA-CSF-treated animals in the Morris water maze (23). Based on these reports, Kersten *et al* (10) hypothesized that anxiety-related behaviors might be enhanced in NMDA-CSF-treated animals. The present study demonstrated that the total distance of horizontal movement was significantly decreased in the NMDA1 group on day 16 after immunization compared with the CON group. This observation is less consistent with previous reports that the total distance during the observation period did not differ between the experimental groups, which suggested that spontaneous motor activity was completely normal (23,31). The spontaneous activity was derived by calculating the total movement distance of mice from 20-60 min in the mining experiment (32). The present study calculated the total horizontal movement distance of mice within 5 min and these results demonstrated an increase in avoidance in the NMDA1 group or an association with depressive behavior. This was consistent with the progressive memory deficits and depression-like behaviors exhibited by the anti-NMDAR encephalitis mouse model previously constructed by Planagumà *et al* (3).

The triggers of the autoimmune response of NMDAR proteins are presently unknown. A previous study reported the use of tetrameric xenopus holoprotein immunogens, NMDA1/GluN2B receptors or rat NMDA1/GluN2A receptors to generate NMDAR antibodies to produce fulminant encephalitis (4). Using the GluN1356-385 peptide that targets the ATD of GluN1, an anti-NMDAR encephalitis model was previously established via active immunization (7). Intranasal infection with herpes simplex virus has also been reported to induce circulating anti-NMDAR antibodies in mice, which may explain the pathogenesis of secondary anti-NMDAR encephalitis in patients with herpes simplex virus encephalitis (5). In the present study, the thin outer segment from the NMDA1 subunit was used as the immunogen, which was adequate to induce high titers of pathogenic anti-NMDA1 autoantibodies. Actively immunized mice developed memory deficits and anxiety-related symptoms typical of mouse anti-NMDAR encephalitis. This active immunization model may be useful for studying NMDAR encephalitis and could aid in further investigations on the pathogenesis of the disease, thus contributing to the development of potential new therapies in the future.

Nonetheless, the present study has certain limitations. Although NMDAR density in the hippocampus of mice immunized with the NMDA1 protein was reduced, the mice did not develop spontaneous seizures. In addition, the role of B and T cells in disease induction is yet to be determined and further studies are warranted.

The present study successfully constructed a mouse model of anti-NMDAR encephalitis. The model mice exhibited symptoms of anxiety, depression and memory impairment and a significant increase in anti-NMDA1 antibodies in the peripheral blood of the mice. Synaptic and total NMDA1 protein expressions were significantly reduced in mouse hippocampus tissue and cultured hippocampal cells. However, the expression of the PSD-95 protein was not significantly different between the control and NMDA1 immunization models.

Acknowledgements

Not applicable.

Funding

This study was funded by the National Natural Science Foundation of China (grant no. 81960233) and the Key Research and Development Project of Ningxia (grant nos. 2018BFG02017 and 2019BCG01003).

Availability of data and materials

The datasets used and/or analyzed during the current study are available from the corresponding author on reasonable request.

Authors' contributions

LY and YW confirm the authenticity of all the raw data. LY contributed to the study planning, data collection, data analysis, statistical analysis, data interpretation and manuscript writing. YW, JY, GW, NZ, XG and JG performed the experimental procedures. ZW contributed to the study conception and design, supervision of data collection and analysis, data interpretation and writing and revising the manuscript. All authors read and approved the final version of the manuscript.

Ethics approval and consent to participate

All procedures involved in this study were approved by the Laboratory Animal Ethical and Welfare Committee of Laboratory Animal Center, Ningxia Medical University (Yinchuan, China; approval no. IACUC-NYLAC-2019-072).

Patient consent for publication

Not applicable.

Competing interests

The authors declare that they have no competing interests.

References

1. Yang J and Liu X: Immunotherapy for refractory autoimmune encephalitis. Front Immunol 12: 790962, 2021.
2. Mikasova L, De Rossi P, Bouchet D, Georges F, Rogemond V, Didelot A, Meissirel C, Honnorat J and Groc L: Disrupted surface cross-talk between NMDA and Ephrin-B2 receptors in anti-NMDA encephalitis. Brain 135: 1606-1621, 2012.
3. Planagumà J, Leypoldt F, Mannara F, Gutiérrez-Cuesta J, Martín-García E, Aguilar E, Titulaer MJ, Petit-Pedrol M, Jain A, Balice-Gordon R, *et al*: Human N-methyl D-aspartate receptor antibodies alter memory and behaviour in mice. Brain 138: 94-109, 2015.
4. Jones BE, Tovar KR, Goehring A, Jalali-Yazdi F, Okada NJ, Gouaux E and Westbrook GL: Autoimmune receptor encephalitis in mice induced by active immunization with conformationally stabilized holoreceptors. Sci Transl Med 11: eaaw0044, 2019.
5. Linnoila J, Pulli B, Armangué T, Planagumà J, Narsimhan R, Schob S, Zeller MWG, Dalmau J and Chen J: Mouse model of anti-NMDA receptor post-herpes simplex encephalitis. Neurol Neuroimmunol Neuroinflamm 6: e529, 2018.
6. Pan H, Oliveira B, Saher G, Dere E, Tapken D, Mitjans M, Seidel J, Wesolowski J, Wakhloo D, Klein-Schmidt C, *et al*: Uncoupling the widespread occurrence of anti-NMDAR1 autoantibodies from neuropsychiatric disease in a novel autoimmune model. Mol Psychiatry 24: 1489-1501, 2019.
7. Ding Y, Zhou Z, Chen J, Peng Y, Wang H, Qiu W, Xie W, Zhang J and Wang H: Anti-NMDAR encephalitis induced in mice by active immunization with a peptide from the amino-terminal domain of the GluN1 subunit. J Neuroinflammation 18: 53, 2021.
8. Lin Y, Liu Z, Jiang J, Jiang Z, Ji Y and Sun B: Expression of intracellular domain of epidermal growth factor receptor and generation of its monoclonal antibody. Cell Mol Immunol 1: 137-141, 2004.
9. Liu B, Kong Q, Zhang D and Yan L: Codon optimization significantly enhanced the expression of human 37-kDa iLRP in *Escherichia coli*. 3 Biotech 8: 210, 2018.
10. Kersten M, Rabbe T, Blome R, Porath K, Sellmann T, Bien CG, Köhling R and Kirschstein T: Novel object recognition in rats with NMDAR dysfunction in CA1 after stereotactic injection of anti-NMDAR encephalitis cerebrospinal fluid. Front Neurol 10: 586, 2019.
11. Graus F, Titulaer MJ, Balu R, Benseler S, Bien CG, Cellucci T, Cortese I, Dale RC, Gelfand JM, Geschwind M, *et al*: A clinical approach to diagnosis of autoimmune encephalitis. Lancet Neurol 15: 391-404, 2016.
12. Hemmer B, Kerschensteiner M and Korn T: Role of the innate and adaptive immune responses in the course of multiple sclerosis. Lancet Neurol 14: 406-419, 2015.
13. Bjelobaba I, Begovic-Kupresanin V, Pekovic S and Lavrnja I: Animal models of multiple sclerosis: Focus on experimental autoimmune encephalomyelitis. J Neurosci Res 96: 1021-1042, 2018.
14. Viegas S, Jacobson L, Waters P, Cossins J, Jacob S, Leite MI, Webster R and Vincent A: Passive and active immunization models of MuSK-Ab positive myasthenia: Electrophysiological evidence for pre and postsynaptic defects. Exp Neurol 234: 506-512, 2012.
15. Castillo-Gómez E, Oliveira B, Tapken D, Bertrand S, Klein-Schmidt C, Pan H, Zafeiriou P, Steiner J, Jurek B, Trippe R, *et al*: All naturally occurring autoantibodies against the NMDA receptor subunit NR1 have pathogenic potential irrespective of epitope and immunoglobulin class. Mol Psychiatry 22: 1776-1784, 2017.
16. Dalmau J, Gleichman AJ, Hughes EG, Rossi JE, Peng X, Lai M, Dessain SK, Rosenfeld MR, Balice-Gordon R and Lynch DR: Anti-NMDA-receptor encephalitis: Case series and analysis of the effects of antibodies. Lancet Neurol 7: 1091-1098, 2008.
17. Hughes EG, Peng X, Gleichman AJ, Lai M, Zhou L, Tsou R, Parsons TD, Lynch DR, Dalmau J and Balice-Gordon RJ: Cellular and synaptic mechanisms of anti-NMDA receptor encephalitis. J Neurosci 30: 5866-5875, 2010.
18. Gleichman AJ, Spruce LA, Dalmau J, Seeholzer SH and Lynch DR: Anti-NMDA receptor encephalitis antibody binding is dependent on amino acid identity of a small region within the GluN1 amino terminal domain. J Neurosci 32: 11082-11094, 2012.
19. Migaud M, Charlesworth P, Dempster M, Webster LC, Watabe AM, Makhinson M, He Y, Ramsay MF, Morris RG, Morrison JH, *et al*: Enhanced long-term potentiation and impaired learning in mice with mutant postsynaptic density-95 protein. Nature 396: 433-439, 1998.
20. He J, Bellini M, Xu J, Castleberry AM and Hall RA: Interaction with cystic fibrosis transmembrane conductance regulator-associated ligand (CAL) inhibits beta1-adrenergic receptor surface expression. J Biol Chem 279: 50190-50196, 2004.
21. Malviya M, Barman S, Golombeck KS, Planagumà J, Mannara F, Strutz-Seebohm N, Wrzos C, Demir F, Baksmeier C, Steckel J, *et al*: NMDAR encephalitis: Passive transfer from man to mouse by a recombinant antibody. Ann Clin Transl Neurol 4: 768-783, 2017.
22. Planagumà J, Haselmann H, Mannara F, Petit-Pedrol M, Grünewald B, Aguilar E, Röpke L, Martín-García E, Titulaer MJ, Jercog P, *et al*: Ephrin-B2 prevents N-methyl-D-aspartate receptor antibody effects on memory and neuroplasticity. Ann Neurol 80: 388-400, 2016.
23. Zhang Q, Tanaka K, Sun P, Nakata M, Yamamoto R, Sakimura K, Matsui M and Kato N: Suppression of synaptic plasticity by cerebrospinal fluid from anti-NMDA receptor encephalitis patients. Neurobiol Dis 45: 610-615, 2012.
24. Naber PA, Witter MP and Lopez da Silva FH: Perirhinal cortex input to the hippocampus in the rat: Evidence for parallel pathways, both direct and indirect. A combined physiological and anatomical study. Eur J Neurosci 11: 4119-4133, 1999.
25. Witter MP, Naber PA and Lopes da Silva F: Perirhinal cortex does not project to the dentate gyrus. Hippocampus 9: 605-606, 1999.
26. Abe H, Ishida Y and Iwasaki T: Perirhinal N-methyl-D-aspartate and muscarinic systems participate in object recognition in rats. Neurosci Lett 356: 191-194, 2004.
27. Winters BD and Bussey TJ: Glutamate receptors in perirhinal cortex mediate encoding, retrieval, and consolidation of object recognition memory. J Neurosci 25: 4243-4251, 2005.
28. Barker GRI, Warburton EC, Koder T, Dolman NP, More JC, Aggleton JP, Bashir ZI, Auberson YP, Jane DE and Brown MW: The different effects on recognition memory of perirhinal kainate and NMDA glutamate receptor antagonism: Implications for underlying plasticity mechanisms. J Neurosci 26: 3561-3566, 2006.

29. Simon P, Dupuis R and Costentin J: Thigmotaxis as an index of anxiety in mice. Influence of dopaminergic transmissions. Behav Brain Res 61: 59-64, 1994.
30. Liu GX, Cai GQ, Cai YQ, Sheng ZJ, Jiang J, Mei Z, Wang ZG, Guo L and Fei J: Reduced anxiety and depression-like behaviors in mice lacking GABA transporter subtype 1. Neuropsychopharmacology 32: 1531-1539, 2007.
31. Li Y, Tanaka K, Wang L, Ishigaki Y and Kato N: Induction of memory deficit in mice with chronic exposure to cerebrospinal fluid from patients with anti-N-Methyl-D-aspartate receptor encephalitis. Tohoku J Exp Med 237: 329-338, 2015.
32. Liu YP, Liu T, Bi H, Zhang L and Dang YH: Effects of strain, sex and circadian rhythm on open field test on mice. Xi'an Jiaotong Daxue Xuebao Yixue Ban 35: 634-638, 2014.